

was shown to stimulate melanogenesis by upregulating the extracellular signal-regulated kinase (ERK) pathway, which induces the expression of tyrosinase via the activation of CREB. In addition to this pathway, nobiletin inhibits phosphodiesterase leading to an elevation of intracellular cAMP levels [14], which bypasses the alpha-MSH pathways.

We previously found that the CREB-specific coactivator TORC1 (transducer of CREB activity, also called CRTC1) and its repressor, salt-inducible-kinase 2 (SIK2) [15,16,17], are fundamental determinants of the melanogenic program in mice [18]. Exposure of B16F10 melanoma cells to UV light results in the immediate nuclear translocation of TORC1, which is inhibited by SIK2. Overexpression of dominant negative TORC1 also inhibits UV-induced *Mitf* gene expression and melanogenesis. alpha-MSH signaling regulates hair pigmentation, and a decrease in alpha-MSH activity in hair follicle melanocytes switches the synthesis of melanin from eumelanin (black) to pheomelanin (yellow). Mice with the lethal yellow allele of agouti (*A^y/a*) have yellow hair due to the impaired activation of the alpha-MSH receptor. *A^y/a* mice with *Siik2*^{-/-} have brown hair, indicating that SIK2 represses eumelanogenesis in mice.

Here we report that flavonoids with an *O*-methyl group at their 4' position efficiently inhibit SIK2 action in cultured melanoma cells and promote the melanogenic program in a TORC1-dependent

manner. Diosmetin (4'-*O*-methylfluteolin) and fisetin (after its conversion into 4'-*O*-methylfisetin *in vivo*) enhance eumelanogenesis in *A^y/a* mice whose CREB-cascades were sensitized by the *Siik2* heterozygous (*Siik2*^{+/-}) background.

Results

SIK2 inhibitory activity of the flavonoids

To identify SIK2 inhibitory substances, we employed an enzyme-linked immunosorbent assay (ELISA) system and screened the compounds using a kinase inhibitor library (BioMol). Most candidates, *e.g.*, staurosporine, hypericin, etc. [19], were non-specific kinase inhibitors and were considered difficult to utilize in structure-activity-related studies. However, quercetin, a flavonoid, has a number of derivatives despite its weak inhibitory activity (IC₅₀ = 500 nM); therefore, we decided to examine the SIK2-inhibitory activity of quercetin derivatives.

The structures of flavonoids (Figure 1A) and their SIK2-inhibitory activity (Figure 1B) are shown. Fisetin was found to inhibit SIK2 even at a low concentration (50 nM). Some of the *O*-methylated derivatives, such as diosmetin, inhibited SIK2 at medium concentrations (50–500 nM).

To monitor the SIK2-inhibitory activity in cultured cells (HEK293), we employed the CRE-reporter assay. As shown in

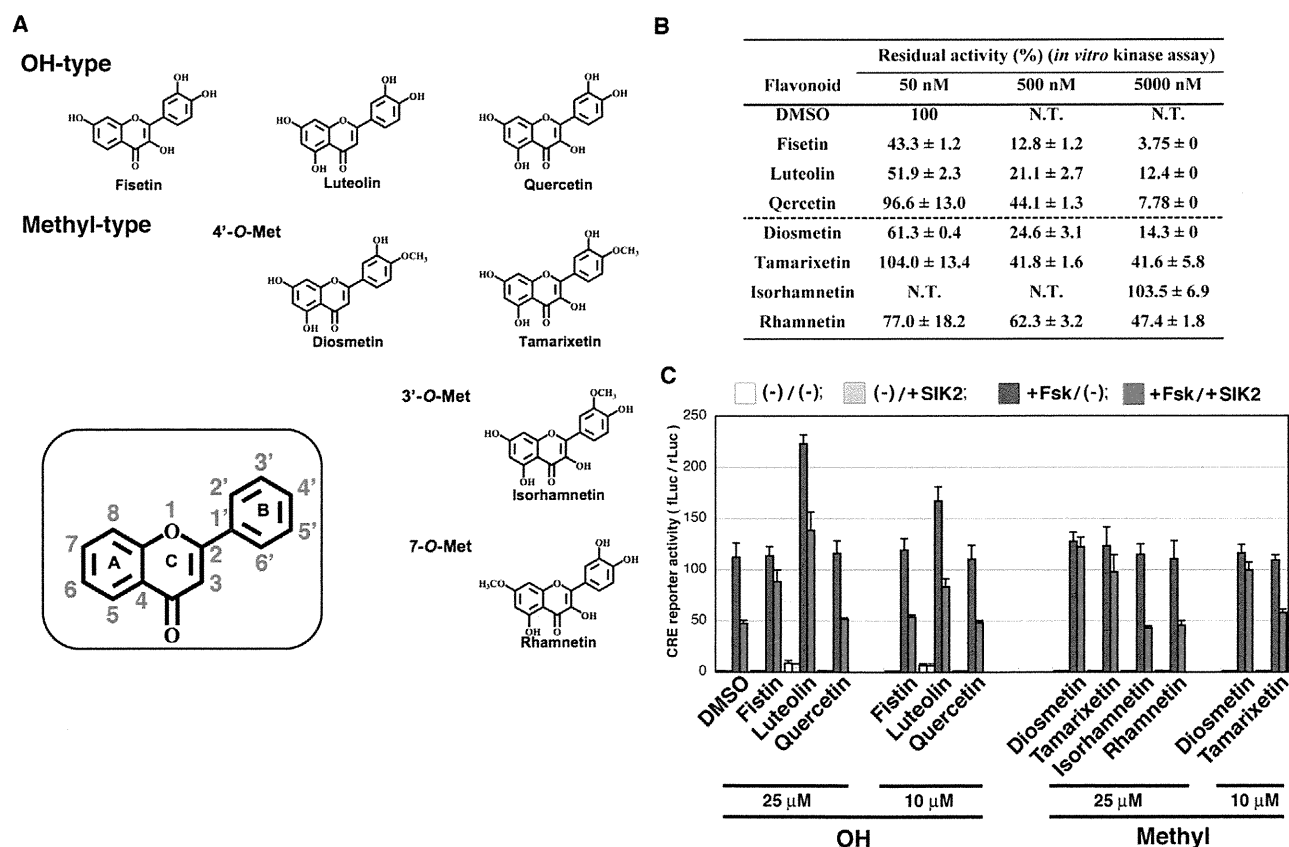


Figure 1. Inhibition of SIK2 by flavonoids. (A) Structure of the flavonoids used in this study. (B) *In vitro* kinase assay of SIK2. GST-SIK2 expressed in COS-7 cells was used as the enzyme, while GST-TORC2 peptide [42], expressed in *Escherichia coli*, was used as the substrate for the ELISA. The optical density (OD) value in the absence of a flavonoid was set as 100%. $n = 2$, means and differences are shown. (C) HEK293 cells transformed with the CRE-Luc firefly luciferase plasmid (200 ng) and pRL-Tk Int- (internal *Renilla* luciferase: 30 ng) in the presence or absence of pTarget-SIK2 (50 ng) were treated with forskolin (Fsk: 20 μM) in the presence of the indicated dose of flavonoids. The ratio of firefly luciferase to *Renilla* luciferase is shown. $n = 2$, means and differences are shown. doi:10.1371/journal.pone.0026148.g001

Figure 1C, 25 μM fisetin inhibited the SIK2-mediated suppression of CRE activity that had been upregulated by the cAMP-agonist forskolin. However, a low dose of fisetin (10 μM) failed to inhibit SIK2 activity in cultured cells, while diosmetin was able to inhibit SIK2 even at a low dose (10 μM), suggesting that other parameters, such as cell permeability, may affect their SIK2-inhibitory activity in cultured cells. On the other hand, it is also important that the *O*-methyl group at the 4'-position of the B-ring more increased their SIK2-inhibitory activity in cultured cells than the *O*-methyl group at the 3'-position or at the 7- position.

O-methyl-flavonoids promote melanogenesis in B16F10 cells

Because one of the representative phenomena of SIK2 inhibition is the promotion of melanogenesis, we employed a melanogenesis assay using B16F10 melanoma cells to evaluate SIK2-inhibitory flavonoids. As shown in Figure 2, non-methylated flavonoids did not induce melanogenesis. In contrast, the 4'-*O*-methyl flavonoids diosmetin and tamarixetin efficiently induced melanogenesis, while the 3'-*O*-methyl flavonoid isorhamnetin had a modest effect. A small induction of melanogenesis was observed when the 7-*O*-methyl flavonoid rhamnetin was added into the cultured medium.

The requirement of the methyl group at the 4'-position of the B-ring for melanogenesis in B16F10 melanoma cells was similar to that for the inhibition of the SIK2-mediated suppression of CREB activity in HEK293 cells, suggesting that 4'-*O*-methyl flavonoids may induce melanogenesis mainly due to the inhibition of SIK2. The effect of fisetin on melanogenesis was not affected by other factors, such as cell-permeability and stability, which are different between cell types, because fisetin did not affect CREB activity in B16F10 melanoma cells (shown later).

Flavonoids promote eumelanogenesis *in vivo*

CREB activity determines the ratio of eumelanogenesis to pheomelanogenesis in hair follicle melanocytes *in vivo*, and inhibition of SIK2 facilitates eumelanogenesis due to the constitutive activation of CREB. Mice with the *lethal yellow* allele of *agouti* (*A*) have yellow hair due to the impaired activation of the alpha-MSH receptor followed by the inactivation of the cAMP-CREB cascade. The *Sik2*^{-/-} genetic background reactivates the CREB cascade in *A/a* mice, which restores the yellow hair color to wild-type mice (brown).

The *Sik2* heterozygous (*Sik2*^{+/-}) background partially restored hair color, but *Sik2*^{+/-}; *A/a* mice were highly sensitive to CREB agonists, such as UV irradiation, which appeared as a hair color change (Figure 3A). Therefore, we decided to use *Sik2*^{+/-}; *A/a* mice to evaluate the effect of flavonoids on melanogenesis *in vivo*. We assessed the activity of fisetin, quercetin, and diosmetin because their low cost would facilitate their use as dietary supplements. As shown in Figure 3B, fisetin and diosmetin changed the hair color of *Sik2*^{+/-}; *A/a* mice, while quercetin had a modest effect. This hair color change was reversible. The difference between fisetin and quercetin could be explained by their inhibitory efficiency toward SIK2 in HEK293 cells (Figure 1C); however, the fact that fisetin promoted eumelanogenesis at the same level as diosmetin disagreed with the results observed in B6F10 melanoma cells (Figure 2). Therefore, we surmised that some of the metabolites, probably *O*-methylfisetin, might promote eumelanogenesis in mice consuming fisetin. To confirm this hypothesis, we analyzed fisetin metabolites in feces and identified mono-methylfisetin in the metabolites (Figure 3C).

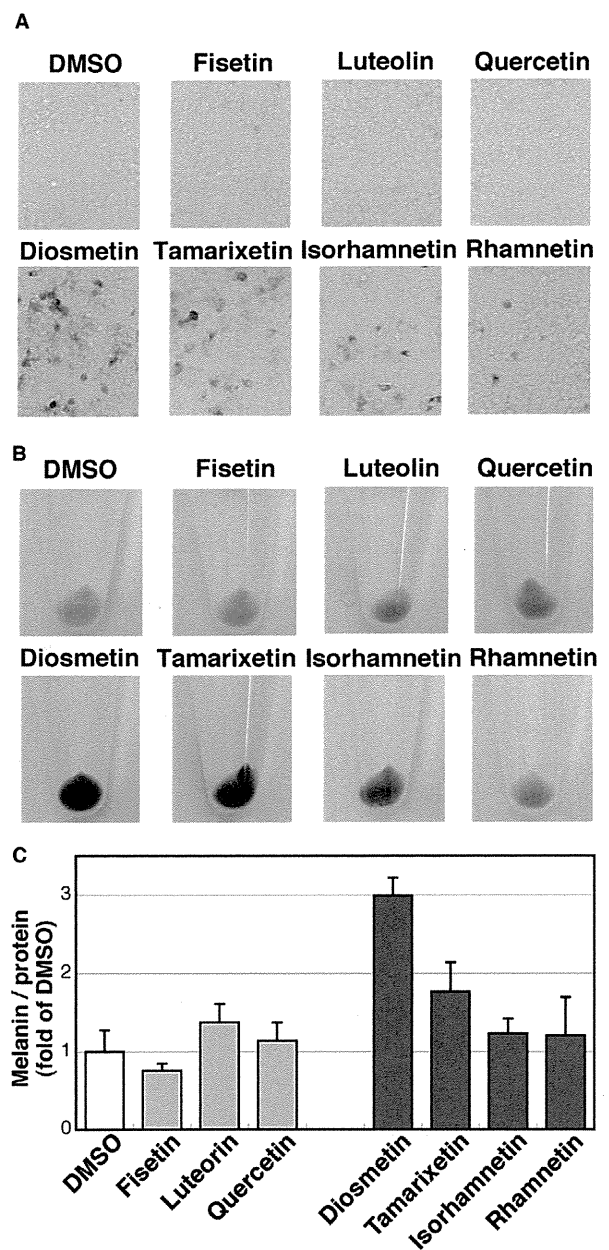


Figure 2. Induction of melanogenesis by flavonoids in B16F10 melanoma cells. (A) B16F10 melanoma cells were treated with 10 μM flavonoids for 3 d with a medium change at day 2. (B) The cells were recovered in test tubes. (C) Melanin was extracted with an alkaline method. After normalization of the melanin content to the protein amount in each sample, the melanin level was expressed as fold of control (DMSO-treated cells). $n=3$, means and standard deviations (S.D.) are shown. doi:10.1371/journal.pone.0026148.g002

4'-*O*-methylfisetin strongly promotes melanogenesis in B16F10 melanoma cells

The LC system is not able to separate 4'-*O*-methyl flavonoids from their 3'-*O*-methyl isomers, and 4'-*O*-methylfisetin is not commercially available, while 3'-*O*-methyl fisetin is available as geraldol. Therefore, we decided to synthesize 4'-*O*-methylfisetin using CH_3I to confirm its potential as a promoter of melanogenesis (Figure 4A). The 4'-OH group of fisetin might more actively

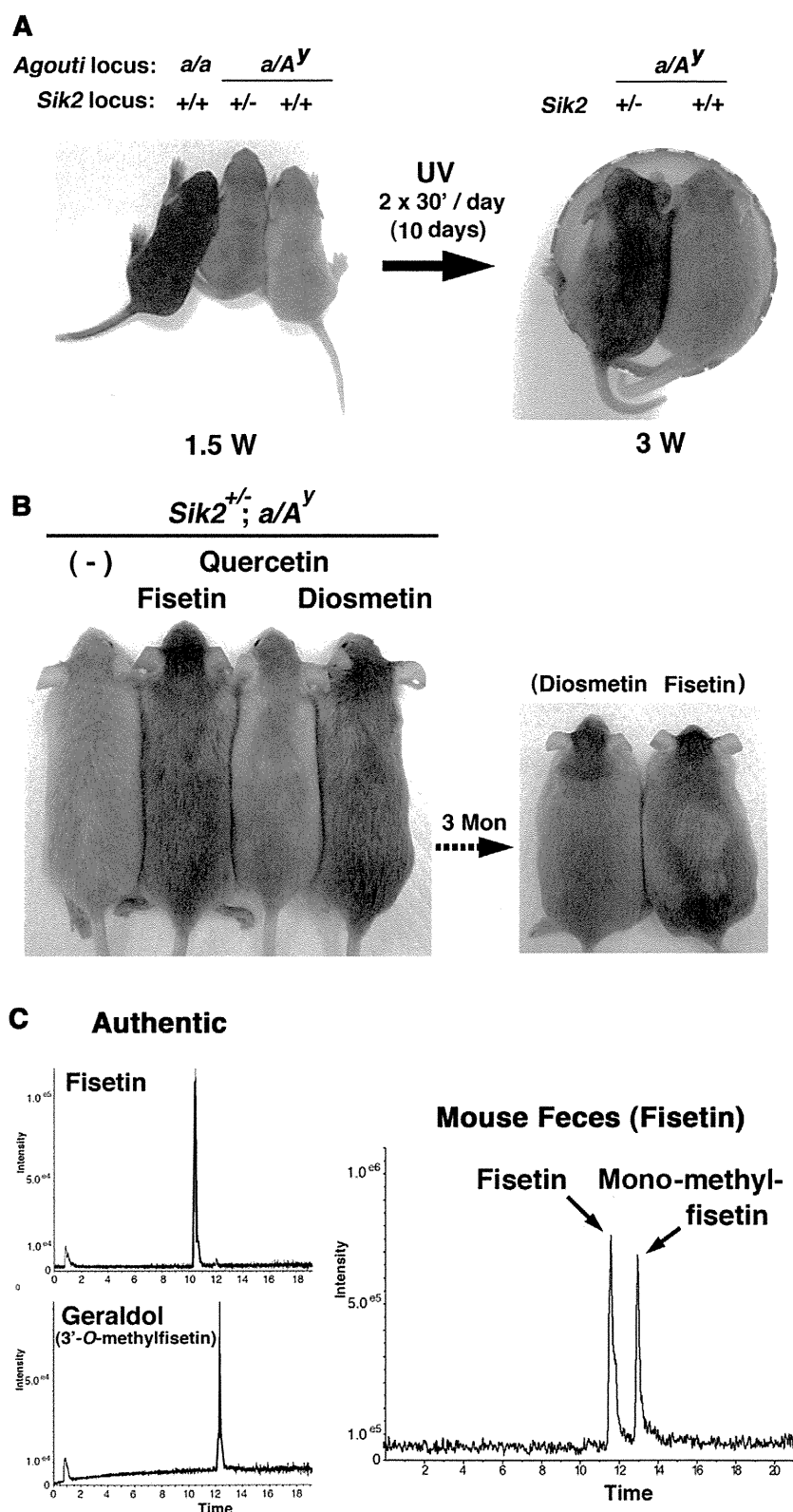


Figure 3. Induction of melanogenesis by flavonoids *in vivo*. (A) 1.5-week-old A^y/a male mice with different *Sik2* backgrounds ($Sik2^{+/+}$ or $Sik2^{+/-}$) exposed to a black lamp (15 W at 20 cm distance) for 30 min twice daily for 10 d. (B) 4-week-old male mice were fed with a diet supplemented with 0.2% flavonoids. After 1 week, the diet was changed to a normal diet (flavonoid free), and the mice were fed for an additional week until all of their hair was replaced by newly grown hair. After a photograph was taken under anesthesia, the mice were fed for a further 3 months until the next set of hair grew. The photographs show a representative mouse from each group (n=4). (C) Flavonoids in feces derived from fisetin-treated mice were extracted with

ethyl acetate and detected by LC-MS with a scan range of ms 285–299, as described in the Materials and Methods. The positions of authentic flavonoids are also shown in left panels.
doi:10.1371/journal.pone.0026148.g003

accept the methyl group than the 3'-OH group did because the yield of 4'-*O*-methylfisetin (5.3%, 5.9 mg) was higher than the 3'-*O*-isomer (<1.0%). The identity of 4'-*O*-methylfisetin was confirmed by ¹H NMR, ¹³C NMR, and ESI-MS [20] (Figure S1).

When 4'-*O*-methylfisetin was added into the culture medium of B16F10 melanoma cells, the SIK2-mediated suppression of CREB activity was weakened (Figure 4B) and melanogenesis was strongly promoted (Figure 4C), suggesting that eumelanogenesis in fisetin-treated mice might be induced by 4'-*O*-methylfisetin.

4'-*O*-methylfisetin promotes melanogenesis dependent on TORC1 and independent of cAMP

To examine the molecular mechanisms underlying 4'-*O*-methylfisetin-induced melanogenesis, we monitored the mRNA expression of the melanogenic genes, M-type *Mitf*, A-type *Mitf*, and *Tyrosinase*. As shown in Figure 5A, 4'-*O*-methylfisetin induced these mRNAs in B16F10 melanoma cells. The Tyrosinase protein level (Tyr) was also elevated in 4'-*O*-methylfisetin-treated cells

(Figure 5B), which was observed from 3 μM. Geraldol was also able to induce Tyrosinase expression, but its efficiency was less than one-third of 4'-*O*-methylfisetin.

When we examined CREB phosphorylation levels (Figure 5B), we noticed that 4'-*O*-methylfisetin induced melanogenesis without elevating the phosphorylation of CREB at Ser133. This was confirmed by an assay indicating that these flavonoids had little effect on intracellular cAMP levels in B16F10 melanoma cells (Figure 5C). In addition to cAMP/PKA cascade, 4'-*O*-methylfisetin did not alter the phosphorylation levels of Erk and GSK-3β, while fisetin and geraldol enhanced pGSK-3β signals (Figure S2).

Since the loss of SIK2 induces melanogenesis by activating TORC1, we monitored the activation of TORC1 by its intracellular distribution. As shown in Figure 5D, 4'-*O*-methylfisetin induced the nuclear accumulation of TORC1, but other flavonoids did not. We then examined whether 4'-*O*-methylfisetin was able to activate CREB, and if so, whether this activation was

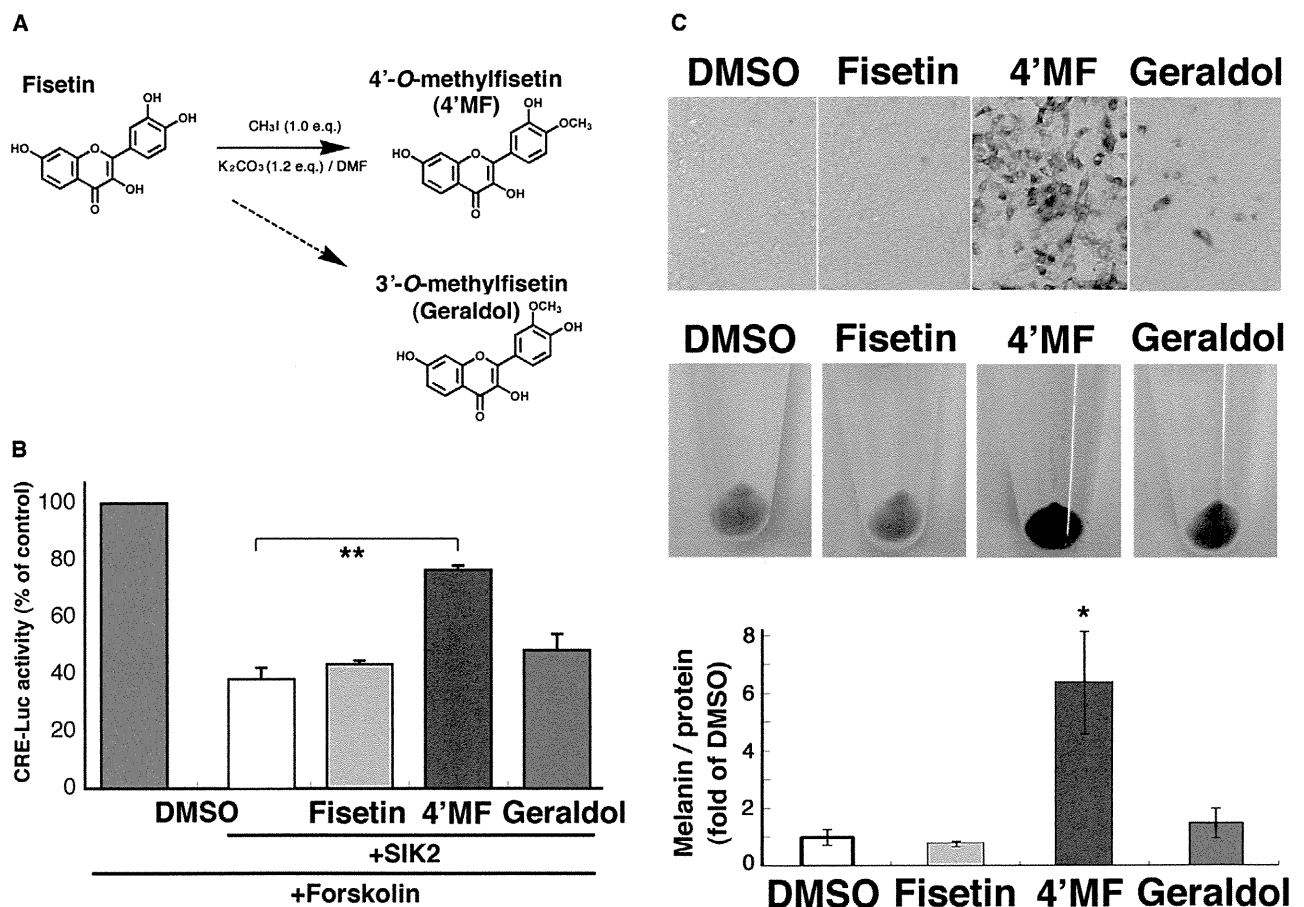


Figure 4. 4'-*O*-methylfisetin (4'MF) inhibits SIK2-mediated CRE suppression and induces melanogenesis in B16F10 melanoma cells. (A) Synthesis of 4'MF. (B) B16F10 melanoma cells transformed with CRE-Luc firefly luciferase plasmid (200 ng) with pRL-Tk Int- (internal *Renilla* luciferase: 30 ng) in the presence or absence of pTarget-SIK2 (50 ng) were treated with forskolin (Fsk: 20 μM) in the presence of the indicated dose of flavonoids. The relative units of firefly luciferase were normalized to *Renilla* luciferase, and expressed as % of control (without flavonoid or SIK2). n = 3, means and S.D. are shown. **, *p* < 0.01. (C) B16F10 melanoma cells were treated with 10 μM flavonoids for 3 d, with a medium change at day 2, and melanin was measured. n = 3, means and S.D. are shown. *, *p* < 0.05.
doi:10.1371/journal.pone.0026148.g004

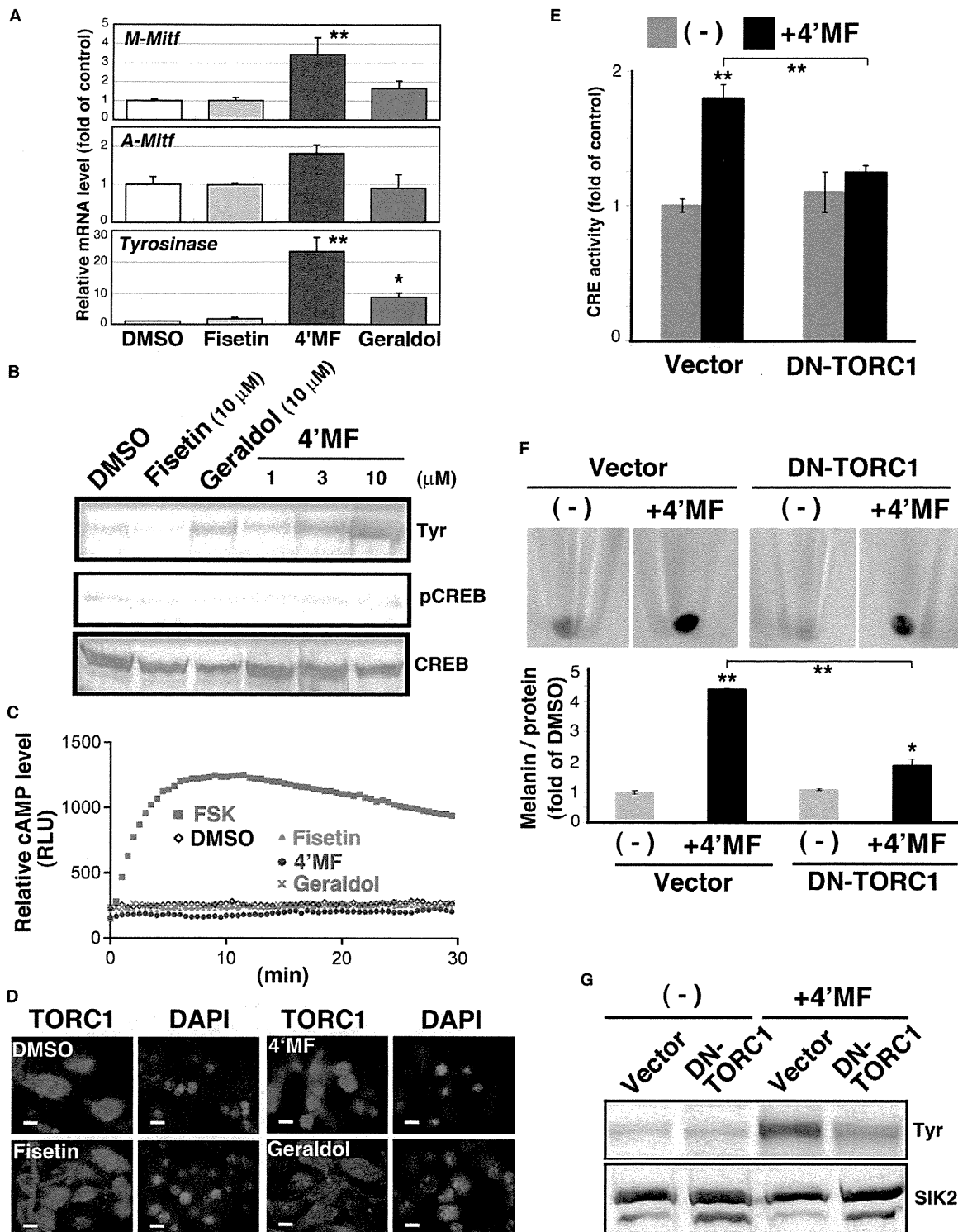


Figure 5. 4'MF induces melanogenesis by activating TORC1 without enhancing the cAMP level in B16F10 melanoma cells. (A) Quantitative PCR analyses were performed with total RNA prepared from flavonoid-treated B16F10 melanoma cells (10 μ M for 3 d, with a medium change at day 2). The mRNA levels are shown as fold of control. $n=3$, means and S.D. are shown. 4'MF: 4'-O-methylfisetin. * and **, $p<0.05$ and <0.01 , respectively. (B) Tyrosinase (Tyr) protein was detected by western blot analysis. 4'MF was added at the indicated concentration. pCREB (pSer133) and total CREB were also examined using the same cell lysate. The panels represent the findings from one of the duplicated experiments. (C) B16F10 cells transfected with the cAMP-indicator plasmid pGloSensor-22F were treated with 10 μ M flavonoid or forskolin (Fsk; 20 μ M) in the presence of luciferin. The relative light units are shown as relative cAMP levels. (D) B16F10 cells were treated with 10 μ M flavonoids for 72 h and then fixed with 4% paraformaldehyde. TORC1 was detected with the anti-TORC1/3 antibody. Nuclei were stained with DAPI. (E) B16F10 melanoma cells transfected with the dominant negative TORC1 (DN-TORC1) adenovirus or empty adenovirus (Vector) were transfected with the CRE-Luc firefly

luciferase plasmid (200 ng) and pRL-Tk Int- (internal *Renilla* luciferase: 30 ng). After 24 h, the cells were treated with 10 μ M 4'-MF for an additional 24 h. CRE activity was expressed as fold of control (the cells were transfected with the empty adenovirus and not treated with 4' MF). n = 3, means and S.D. are shown. Bars indicate 10 μ m. (F) B16F10 melanoma cells transfected with the adenoviruses as in (E) were treated with 10 μ M 4' MF for 3 d with a medium change at day 2, and the melanin content was measured. n = 3, means and S.D. are shown. (G) Tyrosinase protein levels in B16F10 melanoma cells (the same sample as in F) were examined by western blot analyses. SIK2 was detected as a loading control.
doi:10.1371/journal.pone.0026148.g005

dependent on TORC1. Expectedly, 4'-*O*-methylfisetin upregulated CRE-reporter activity, which was inhibited by the overexpression of DN-TORC1.

Finally, we tested whether DN-TORC1 was able to inhibit 4'-*O*-methylfisetin-induced melanogenesis. As shown in Figure 5E, DN-TORC1 inhibited melanin synthesis (Figure 5F), which was accompanied by the suppression of Tyrosinase expression (Figure 5G). These results suggest that 4'-*O*-flavonoids, especially 4'-*O*-methylfisetin, are potent inhibitors of SIK2 and capable of activating TORC1 followed by the induction of the melanogenic program in mice.

Discussion

We have shown that 4'-*O*-methyl flavones can inhibit SIK2 activity and promote melanogenesis via the activation of TORC1 in B16F10 melanoma cells [18]. However, first, we have to discuss about the discrepancy found between the *in vitro* and cultured cell assays for structure activity correlation. The *in vitro* kinase assay using the TORC peptide suggested that non-methylated flavones more potently inhibited SIK2 than their methylated derivatives. However, in HEK293 cells and B16F10 melanoma cells, 4'-*O*-methylflavone inhibited SIK2 more efficiently, suggesting several mechanisms exist by which flavones can inhibit SIK2 in cultured cells. This hypothesis is also supported by the observation that 3'-*O*-methylflavones, such as isorhamnetin and geraldol, do not inhibit SIK2 *in vitro*, while they weakly induce melanogenesis in B16F10 melanoma cells. These results suggested that methylated flavonoids induce the melanogenic program by several mechanisms, such as enhanced cell permeability and SIK2-independent signaling pathways.

Meanwhile, it was also true that the efficiency of SIK2 inhibition and the potency of melanogenic promotion by 4'-*O*-methylflavones in cultured cells (4'-*O*-methylfisetin > diosmetin > tamarixetin) correlated well with the efficiency of SIK2-kinase inhibition *in vitro* by their non-methylated cognates (fisetin > luteolin > quercetin). Moreover, fisetin promoted eumelanogenesis in *A⁺/a⁻; SIK2^{+/-}* mice more potently than quercetin, suggesting that a synergistic effect between the direct inhibition of SIK2 by a structural dependence of flavones and an indirect effect via a mechanism depending on their 4'-*O*-methoxy groups may efficiently promote melanogenesis in mice.

A number of factors and related compounds have been reported to intricately modulate the melanogenic program. For example, tyrosine kinases and glycogen synthase kinase 3 beta (GSK-3 beta) play opposing roles in the regulation of melanogenesis in melanocytes [21]. The transcriptional activity of the MITF protein is modulated by protein kinase cascades that are induced by the stem cell factor and its receptor kinase c-KIT. The activation of c-KIT invokes two opposing pathways: the RAS-RAF-MEK and PI3K-AKT pathways. The RAS-RAF-MEK pathway activates ERK-p90RSK, which phosphorylates CREB at Ser133 and MITF at Ser73 and Ser409 [22] and promotes melanogenesis, whereas AKT inhibits the MITF-activating kinase GSK-3 beta and downregulates melanogenesis [23]. The plant steroid diosgenin also inhibits melanogenesis by activating PI3K signaling [24].

However, the action of GSK-3 beta in the regulation of melanogenesis is complicated and paradoxical. The promoter activity of the *Mitf* gene is upregulated by the beta-catenin-TCF/LEF complex [25], and the phosphorylation of beta-catenin by GSK-3 beta [26] destabilizes beta-catenin and leads to the suppression of MITF-induced melanogenesis [27]. The observation that indirubin derivatives, potent inhibitors of GSK-3 beta [27,28], stabilize the beta-catenin-TCF/LEF complex and promote melanogenesis in B16F10 melanoma cells suggests that *Mitf* expression, rather than the phosphorylation-dependent activation of MITF, is the rate-limiting step of the melanogenic program [29].

The GSK-3 beta-mediated regulation of melanogenesis is often accompanied by the activation of the cAMP-PKA-CREB pathway. The plant steroid glycyrrhizin inhibits GSK-3 beta activity, while stimulating CREB-mediated transcription by activating PKA, which results in the promotion of melanogenesis [30]. Meanwhile, we reported that the GSK-3 beta inhibitor indirubin induces the degradation of SIK1 and SIK2 proteins in COS-7 cells [31] and in differentiating C2C12 myocytes [32]. GSK-3 beta is capable of phosphorylating (activating) sites in the activation loop of SIK1/2, and the activated SIK1/2 proteins are stable [31], suggesting that B16F10 melanoma cells that have been treated with GSK-3 beta inhibitors have low levels of SIK2, which would promote melanogenesis. Meanwhile, 4'-*O*-methylfisetin did not modulate the AKT-GSK-3 beta and MEK cascades, suggesting that the melanogenic programs induced by 4'-*O*-methylflavones may be different from those induced by plants compounds modulating the AKT-GSK-3 beta and MEK cascades.

Some methylated flavonoids, such as nobletin [14] and ayanin [33], inhibit phosphodiesterase, which increases the intracellular cAMP levels [34]. In contrast to these polymethylated flavonoids, 4'-*O*-methylfisetin elevates neither CREB phosphorylation levels nor cAMP-indicator luciferase activity, irrespective of the length of treatment, suggesting that 4'-*O*-methylfisetin upregulates CREB activity independently of cAMP. The mechanism of 4'-*O*-methylfisetin-induced CREB activity may depend on the activity of TORC1 induced by SIK2 inhibition.

TORC1, or its other isoforms, plays important roles in neuronal activity, such as memory in the hippocampus [35,36], behavior (food intake) in the arcuate and ventromedial nuclei [37], and corticotrophin-releasing hormone synthesis in the hypothalamus [38]. In addition to these roles, we also found that TORC1 is essential for neuronal survival after brain ischemia [19], which is evident in *SIK2^{-/-}* mice. Interestingly, fisetin was found to enhance memory function in the brain and long term potentiation in cultured PC12 cells via MEK-ERK-mediated CREB activation [39]. Because 4'-*O*-methylfisetin did not activate ERK in B16F10 melanoma cells, the upregulation of TORC activity by SIK2 inhibition has been suggested to be a beneficial strategy for the treatment of neuronal diseases, and fisetin or 4'-*O*-methylfisetin may be helpful to perform this strategy.

On the other hand, the present study also revealed that heterozygous insufficiency of the *SIK2* allele increases the sensitivity of CREB-mediated gene expression *in vivo*, such as switching to eumelanogenesis in hair melanocytes. This phenomenon may be

helpful to screen CREB activators *in vivo*. Given that the daily food intake of A^p/a mice is ~ 4 g on average, the present dose of fisetin, 400 mg/kg, is not extremely high. Unfortunately, fisetin intake elevates the blood glucose levels of A^p/a mice, while diosmetin did slightly (data not shown). As there was no significant difference in blood glucose levels between wild-type and $SiK2^{-/-}$ mice [18,40], fisetin may affect blood glucose homeostasis in a SIK2-independent manner.

In conclusion, by modulating SIK2 signaling, we were able to identify a biologically active substance, 4'-*O*-methylfisetin, which initiated CREB-mediated transcription via TORC1 activation. In this study, we also found that the hair color of $SiK2^{+/-}$ mice and the analysis of metabolites in their feces and blood may act as beneficial indicators to develop compounds that modulate CREB activity.

Materials and Methods

Flavonoids

Luteolin, diosmetin, quercetin, tamarixetin, isorhamnetin, rhamnetin, and geraldol were obtained from Extrasynthese (Genay Cedex, France). Fisetin and forskolin were purchased from Wako Pure Chemicals Co. Ltd., (Osaka, Japan) and Sigma-Aldrich (St. Louis, MO, USA), respectively. These compounds were dissolved in dimethyl sulfoxide (DMSO) as $\times 1000$ stock solutions.

Cell culture, flavonoid treatment, and melanin measurement

B16F10 murine melanoma cells and HEK293 cells were obtained from the American Type Culture Collection (Manassas, VA, USA). B16F10 cells were grown at 37°C under 5% CO₂ in Dulbecco's modified Eagle's medium (DMEM; high glucose) (Wako) supplemented with 10% fetal bovine serum (FBS), penicillin (100 U/mL), and streptomycin (50 μ g/mL). HEK293 cells were grown at 37°C under 5% CO₂ in DMEM (low glucose) (Wako) supplemented with 10% FBS and penicillin/streptomycin.

B16F10 were seeded in 6-well plates at a density of 3.4×10^5 cells/well. After 24 h, the culture medium was replaced with fresh medium supplemented with flavonoids, and, after 48 h, the medium was changed again with fresh medium containing the same flavonoids. After an additional 24 h, the cells were harvested for the melanin or mRNA/protein assays.

To measure melanin, the cells were washed twice with phosphate-buffered saline (PBS), suspended in PBS, and recovered by centrifugation at 8,000 rpm for 1.5 min. The cell pellet was suspended in 300 μ L of 1 N NaOH and incubated at 45°C for 2 h, and, then, melanin was extracted with a chloroform-methanol mixture (2:1). Melanin was detected with a spectrophotometer (BIO-RAD Model 680 MICRO PLATE READER; Bio-Rad, Hercules, CA, USA) at 405 nm. The standard curve was obtained by using purified melanin (0–1000 μ g/mL). The protein concentration of the cell pellets was determined using the Bradford reagent (Bio-Rad) and used for normalization of the melanin content.

Animal experiments and liquid chromatography-mass spectrometry (LC-MS) analysis of flavonoids

The experimental protocols for mice were approved by the committee at the National Institute of Biomedical Innovation (approval ID: DS20-55). $SiK2^{+/-}$; A^p mice (4-week-old male mice; the mice were gifts from ProteinExpress Co. Ltd., Chiba, Japan) were housed under standard light (08:00–20:00) and temperature (23°C/60% humidity) conditions.

Mice feces (3.0 g dry weight) were soaked in water : ethyl acetate (1:1), and the flavonoids were recovered from the organic phase. Ethyl acetate was evaporated under N₂ gas, and the dried residues were dissolved in 25% acetonitrile/water and subjected to LC-MS analysis (API 3000 mass spectrometer; Applied Biosystems, Foster City, CA, USA). To separate the flavonoids, a C₁₈ column (2.0 \times 50 mm i.d., particle size 5 μ m) (Nacalai tesque, Kyoto, Japan) was used. A linear gradient was prepared with 0.1% formic acid in water (solvent A) and acetonitrile (solvent B); from 20% solvent B to 100% solvent B in 25 min at 30°C. The flavonoids were monitored by a UV detector at 255 nm.

Synthesis of 4'-*O*-methylfisetin

The methods for the synthesis of methylflavonoids were described in [41]. To a solution of fisetin (122.4 mg, 4.3×10^{-4} mol) in *N,N*-dimethylformamide (10 ml) was added CH₃I (26.4 μ L, 4.3×10^{-4} mol), and K₂CO₃ (71.7 mg, 5.1×10^{-4} mol). After being stirred for 14 h at room temperature, the reaction mixture was concentrated in vacuo, dissolved in ethyl acetate, washed with sat NaCl, dried over Na₂SO₄ and evaporated. The resulting residue was separated with preparative SiO₂ thin layer chromatography (eluent: chloroform/methanol (9/1)) followed by HPLC using a gel filtration column, JAIGEL GS-320 (Japan Analytical Industry Co., Ltd, Tokyo, Japan) with an eluent methanol, and finally 4'-*O*-methylfisetin was recovered as yellow crystals (5.9 mg, 5.3% yield). The identity and structure of 4'-*O*-methylfisetin was confirmed with electrospray ionization mass spectroscopy (ESI-MS) and ¹H and ¹³C nuclear magnetic resonance (NMR) [20], respectively. 4'-*O*-methylfisetin (C₁₆H₁₃O₆): ¹H NMR (399.65 MHz, CD₃OD) δ : 3.94 (1 H, d, $J=3.6$ Hz), 6.91 (2 H, m), 7.06 (1 H, d, $J=8.4$ Hz), 7.77 (1 H, m), 7.98 (1 H, d, $J=9.6$ Hz). ¹³C NMR (399.65 MHz, CD₃OD): 56.35 (OCH₃) 102.98, 112.24, 115.45, 115.65, 116.08, 121.45, 127.55, 147.42, 150.61, 158.57. The spectral data of 4'-*O*-methylfisetin and its derivatives is shown in Figure S1.

ESI-MS spectra were measured on AB SCIEX API-3000 mass spectrometer. NMR signal was recorded on a JEOL JNM-JSX400 spectrometer using CD₃OD as a solvent and tetramethylsilane (TMS) as the internal standard.

Quantitative real-time PCR

Total RNA was isolated from B16F10 cells by using the EZ1 RNA Universal Tissue Kit (QIAGEN, Venlo Park, the Netherlands), according to the manufacturer's protocol. cDNA was synthesized using the Transcriptor cDNA First Strand Synthesis Kit (Roche Diagnostics Corp., Indianapolis, IN, USA). PCR amplification was performed using Platinum Quantitative PCR SuperMix (Invitrogen). The resulting cDNA was amplified using the specific primers: GAPDH-F, 5'-ACTCACGGCAAATTC AACGG and GAPDH-R, 5'-GACTCCACGACATACTGAGC; Tyrosinase-F, 5'-TGGGGATGAGAAGTTCCTGACTG and Tyrosinase-R, 5'-ACGTAA-TAGTGGTCCCTCAGGT; A-Mitf-F, 5'-GGAAATGCTAGAA-TACAGTCACTA and Pan-Mitf-R, 5'-GTCGCCAGGCTG-GTTTGGACA; and M-Mitf-F 5'-GGAAATGCTAGAA-TACAGTCACTA and Pan-Mitf-R. The reactions were performed for 42 cycles at 95°C for 20 s, 58°C for 20 s, 72°C for 20 s, and 31 cycles at 75°C for 10 s.

Western blot analysis

B16F10 melanoma cells were washed with PBS and lysed with lysis buffer (150 mM Tris (pH 6.8), 60% sodium dodecyl sulfate (SDS), 30% glycerol, and 10% mercaptoethanol). Cell lysates were boiled for 15 min at 95°C and subjected to 10% SDS-polyacrylamide gel electrophoresis and transferred onto polyvinylidene fluoride membranes (Millipore, Bedford, MA, USA). The

membranes were blocked with Blocking-One (Nacalai tesque, Kyoto, Japan) and then incubated with the following primary antibodies: anti-Tyrosinase goat polyclonal antibody (Santa Cruz Biotechnology, Santa Cruz, CA, USA), anti-SIK2 rabbit polyclonal antibody [15], and anti-CREB and anti-phospho CREB rabbit polyclonal antibodies (Cell Signaling Technology, MA, USA) at 4°C overnight. After washing, the membranes were incubated with peroxidase-conjugated secondary antibody at room temperature for 4 h. Detection was performed using the KONICA MINOLTA immunostaining HRP-1000 Kit (KONICA MINOLTA, Tokyo, Japan).

Immunocytochemistry

To perform immunocytochemistry, B16F10 cells were seeded on glass cover-slips. The medium was changed with fresh medium supplemented with 10 μM flavonoid for 72 h. The cells were fixed with 4% formaldehyde and stained with the anti-TORC1/3 rabbit polyclonal antibody. To detect the TORC1-antibody complex, anti-rabbit IgG conjugated with Alexa Fluor-594 (Eugene, OR, USA) was used. Nuclei were stained with 4', 6-diamino-2-phenylindole (DAPI).

Expression vector, adenoviruses, transfection, and luciferase/cAMP assay

The reporter plasmids and adenoviruses were previously described [42,43]. Briefly, B16F10 cells in a 24-well plate were co-transfected with the pTAL-CRE vector (200 ng/well) with the internal reporter pRL-TK (30 ng) in the presence or absence of the SIK2 expression vector (pTarget-SIK2 50 ng) using Lipofectamine2000 (Invitrogen, Carlsbad, CA, USA). After 24 h, the cells were treated with forskolin (20 μM) and cultured for an additional 6 h. Reporter activity was monitored using the Dual Luciferase Reporter Assay Kit (Promega, Madison, WI, USA).

The dominant negative TORC1 (DN-TORC1) adenovirus was previously described [19]. B16F10 cells plated in 6-well dishes were infected with adenoviruses (DN-TORC1 or lacZ at a multiplicity of infection of 10). After a 3 h incubation, the medium was changed with new medium that did not contain adenoviruses, and the cells were cultured for 72 h with a medium change after 48 h.

Fluctuation of the intracellular cAMP level was monitored by the PKA regulatory subunit-like luciferase reporter system, the GloSensor™ cAMP Assay kit (Promega). Briefly, B16F10 cells

were seeded in 96-well plate at a density of 5×10^3 cells/well and incubated for 24 h and transfected with the pGloSensor™-22F cAMP-reporter plasmid (1 ng/well) using LipofectAMIN2000. After 18 h, cells were incubated with GloSensor™ cAMP reagent for 2 h, and, then, forskolin (20 μM) or flavonoids (10 μM) was added into the culture medium.

Statistical analysis

Student's *t*-test was used to assess all experimental data in Microsoft Excel. The mean and standard deviation (S.D.) are shown.

Supporting Information

Figure S1 NMR analysis of 4'-O-methylfisetin and its derivatives (authentic). The structure of 4'-O-methylfisetin was confirmed by comparison of its ¹³C-NMR chemical shifts in B-ring positions with those of other similar flavonoids owing 4'-OH or 4'-OMe with 3'-OMe or 3'-OH groups. ¹³C-NMR chemical shifts of 4'-O-methylfisetin for the B-ring positions, from C-1' to 6', are similar to those of (4'-OMe, 3'-OH)-type tamarixetin [20] and different from those of (4'-OH, 3'-OMe)-type isorhamnetin and geraldor.

(TIF)

Figure S2 4'-O-methylfisetin (4'MF) does not affect the MEK or GSK-3 beta pathways. B16F10 cells cultured in FCS-free medium overnight were treated with fisetin, 4'MF, or geraldol (10 mM) for 30 min. MEK/pMEK and GSK-3 beta/pGSK-3 beta were examined. The photographs indicate a representative set from the duplicate experiments.

(TIF)

Acknowledgments

We are grateful to Mrs. Junko Morita (NIBIO), Ms. Yuko Shimono, Ms. Tomoko Onishi, Mr. Yuki Shiota, and Mr. Akihiro Hojyo (Kansai University) for their technical assistance. We thank ProteinExpress Co. Ltd. (Chiba, Japan) for their providing us *SiK2*^{-/-} mice.

Author Contributions

Conceived and designed the experiments: HT. Performed the experiments: AK. Analyzed the data: KK SU HK YN. Contributed reagents/materials/analysis tools: NH YS TU TS YI YH KU. Wrote the paper: HT.

References

- Lin JY, Fisher DE (2007) Melanocyte biology and skin pigmentation. *Nature* 445: 843–850.
- Hocker TL, Singh MK, Tsao H (2008) Melanoma genetics and therapeutic approaches in the 21st century: moving from the benchside to the bedside. *J Invest Dermatol* 128: 2575–2595.
- Yamaguchi Y, Hearing VJ (2009) Physiological factors that regulate skin pigmentation. *Biofactors* 35: 193–199.
- Vachtenheim J, Borovansky J (2010) “Transcription physiology” of pigment formation in melanocytes: central role of MITF. *Exp Dermatol* 19: 617–627.
- Busca R, Ballotti R (2000) Cyclic AMP a key messenger in the regulation of skin pigmentation. *Pigment Cell Res* 13: 60–69.
- D'Orazio JA, Nobuhisa T, Cui R, Arya M, Spry M, et al. (2006) Topical drug rescue strategy and skin protection based on the role of Mc1r in UV-induced tanning. *Nature* 443: 340–344.
- Jimbou K, Alena F, Dixon W, Hara H (1992) Regulatory factors of pheo- and eumelanogenesis in melanogenic compartments. *Pigment Cell Res Suppl* 2: 36–42.
- Winkel-Shirley B (2002) Biosynthesis of flavonoids and effects of stress. *Curr Opin Plant Biol* 5: 218–223.
- Kovacic P, Somanathan R (2011) Cell signaling and receptors with resorcinols and flavonoids: redox, reactive oxygen species, and physiological effects. *J Recept Signal Transduct Res* 31: 265–270.
- Nakayama T (1994) Suppression of hydroperoxide-induced cytotoxicity by polyphenols. *Cancer Res* 54: 1991s–1993s.
- Shoji T, Masumoto S, Moriichi N, Kobori M, Kanda T, et al. (2005) Procyanidin trimers to pentamers fractionated from apple inhibit melanogenesis in B16 mouse melanoma cells. *J Agric Food Chem* 53: 6105–6111.
- Fujii T, Saito M (2009) Inhibitory effect of quercetin isolated from rose hip (*Rosa canina* L.) against melanogenesis by mouse melanoma cells. *Biosci Biotechnol Biochem* 73: 1989–1993.
- Yoon HS, Lee SR, Ko HC, Choi SY, Park JG, et al. (2007) Involvement of extracellular signal-regulated kinase in nobiletin-induced melanogenesis in murine B16/F10 melanoma cells. *Biosci Biotechnol Biochem* 71: 1781–1784.
- Nagase H, Omac N, Omori A, Nakagawasai O, Tadano T, et al. (2005) Nobiletin and its related flavonoids with CRE-dependent transcription-stimulating and neuritegenic activities. *Biochem Biophys Res Commun* 337: 1330–1336.
- Horike N, Takemori H, Katoh Y, Doi J, Min L, et al. (2003) Adipose-specific expression, phosphorylation of Ser794 in insulin receptor substrate-1, and activation in diabetic animals of salt-inducible kinase-2. *J Biol Chem* 278: 18440–18447.
- Katoh Y, Takemori H, Min L, Muraoka M, Doi J, et al. (2004) Salt-inducible kinase-1 represses cAMP response element-binding protein activity both in the nucleus and in the cytoplasm. *Eur J Biochem* 271: 4307–4319.
- Screaton RA, Conkright MD, Katoh Y, Best JL, Canettieri G, et al. (2004) The CREB coactivator TORC2 functions as a calcium- and cAMP-sensitive coincidence detector. *Cell* 119: 61–74.

18. Horike N, Kumagai A, Shimono Y, Onishi T, Itoh Y, et al. (2010) Downregulation of SIK2 expression promotes the melanogenic program in mice. *Pigment Cell Melanoma Res* 23: 809–819.
19. Sasaki T, Takemori H, Yagita Y, Terasaki Y, Uebi T, et al. (2011) SIK2 is a key regulator for neuronal survival after ischemia via TORC1-CREB. *Neuron* 69: 106–119.
20. Blasko G, Shieh HL, Pezzuto JM, Cordell GA (1989) ¹³C-nmr spectral assignment and evaluation of the cytotoxic potential of rotenone. *J Nat Prod* 52: 1363–1366.
21. Blume-Jensen P, Jiang G, Hyman R, Lee KF, O’Gorman S, Hunter T (2000) Kit/stem cell factor receptor-induced activation of phosphatidylinositol 3’-kinase is essential for male fertility. *Nat Genet* 24: 157–162.
22. Wu M, Hemesath TJ, Takemoto CM, Horstmann MA, Wells AG, et al. (2000) c-Kit triggers dual phosphorylations, which couple activation and degradation of the essential melanocyte factor *Mi*. *Genes Dev* 14: 301–312.
23. Oka M, Nagai H, Ando H, Fukunaga M, Matsumura M, et al. (2000) Regulation of melanogenesis through phosphatidylinositol 3-kinase-Akt pathway in human G361 melanoma cells. *J Invest Dermatol* 115: 699–703.
24. Lee J, Jung K, Kim YS, Park D (2007) Diosgenin inhibits melanogenesis through the activation of phosphatidylinositol-3-kinase pathway (PI3K) signaling. *Life Sci* 81: 249–254.
25. Takeda K, Yasumoto K, Takada R, Takada S, Watanabe K, et al. (2000) Induction of melanocyte-specific microphthalmia-associated transcription factor by Wnt-3a. *J Biol Chem* 275: 14013–14016.
26. Meijer L, Skaltsounis AL, Magiatis P, Polychronopoulos P, Knockaert M, et al. (2003) GSK-3-selective inhibitors derived from Tyrian purple indirubins. *Chem Biol* 10: 1255–1266.
27. Bellei B, Flori E, Izzo E, Maresca V, Picardo M (2008) GSK3beta inhibition promotes melanogenesis in mouse B16 melanoma cells and normal human melanocytes. *Cell Signal* 20: 1750–1761.
28. Cho M, Ryu M, Jeong Y, Chung YH, Kim DE, et al. (2009) Cardamonin suppresses melanogenesis by inhibition of Wnt/beta-catenin signaling. *Biochem Biophys Res Commun* 390: 500–505.
29. Khaled M, Larribere L, Bille K, Aberdam E, Ortonne JP, et al. (2002) Glycogen synthase kinase 3beta is activated by cAMP and plays an active role in the regulation of melanogenesis. *J Biol Chem* 277: 33690–33697.
30. Lee J, Jung E, Park J, Jung K, Park E, et al. (2005) Glycyrrhizin induces melanogenesis by elevating a cAMP level in b16 melanoma cells. *J Invest Dermatol* 124: 405–411.
31. Hashimoto YK, Satoh T, Okamoto M, T H (2008) Importance of autophosphorylation at Ser186 in the A-loop of salt inducible kinase 1 for its sustained kinase activity. *J Cell Biochem* 104: 1724–1739.
32. Takemori H, Katoh Hashimoto Y, Nakae J, Olson EN, Okamoto M (2009) Inactivation of HDAC5 by SIK1 in AICAR-treated C2C12 myoblasts. *Endocr J* 56: 121–130.
33. Chan AL, Huang HL, Chien HC, Chen CM, Lin CN, et al. (2008) Inhibitory effects of quercetin derivatives on phosphodiesterase isozymes and high-affinity [(3) H]-rolipram binding in guinea pig tissues. *Invest New Drugs* 26: 417–424.
34. Peluso MR (2006) Flavonoids attenuate cardiovascular disease, inhibit phosphodiesterase, and modulate lipid homeostasis in adipose tissue and liver. *Exp Biol Med (Maywood)* 231: 1287–1299.
35. Zhou Y, Wu H, Li S, Chen Q, Cheng XW, et al. (2006) Requirement of TORC1 for late-phase long-term potentiation in the hippocampus. *PLoS One* 1: e16.
36. Li S, Zhang C, Takemori H, Zhou Y, Xiong ZQ (2009) TORC1 regulates activity-dependent CREB-target gene transcription and dendritic growth of developing cortical neurons. *J Neurosci* 29: 2334–2343.
37. Altarejos JY, Goebel N, Konkright MD, Inoue H, Xie J, et al. (2008) The Creb1 coactivator *Crtc1* is required for energy balance and fertility. *Nat Med* 14: 1112–1117.
38. Liu Y, Coello AG, Grinevich V, Aguilera G (2010) Involvement of transducer of regulated cAMP response element-binding protein activity on corticotropin releasing hormone transcription. *Endocrinology* 151: 1109–1118.
39. Maher P, Akaishi T, Abe K (2006) Flavonoid fisetin promotes ERK-dependent long-term potentiation and enhances memory. *Proc Natl Acad Sci U S A* 103: 16568–16573.
40. Muraoka M, Fukushima A, Viengchareun S, Lombes M, Kishi F, et al. (2009) Involvement of SIK2/TORC2 signaling cascade in the regulation of insulin-induced PGC-1alpha and UCP-1 gene expression in brown adipocytes. *Am J Physiol Endocrinol Metab* 296: E1430–E1439.
41. Bouktaib M, Lebrun S, Atmani A, Rolando C (2002) Hemisynthesis of all the O-monomethylated analogues of quercetin including the major metabolites, through selective protection of phenolic functions. *Tetrahedron* 58: 10001–10009.
42. Katoh Y, Takemori H, Lin XZ, Tamura M, Muraoka M, et al. (2006) Silencing the constitutive active transcription factor CREB by the LKB1-SIK signaling cascade. *Febs J* 273: 2730–2748.
43. Uebi T, Tamura M, Horike N, Hashimoto YK, Takemori H (2010) Phosphorylation of the CREB-specific coactivator TORC2 at Ser(307) regulates its intracellular localization in COS-7 cells and in the mouse liver. *Am J Physiol Endocrinol Metab* 299: E413–E425.

認知症の病態進展における インスリン抵抗性の役割

里 直行, 武田朱公, 内尾-山田こずえ, 樂木宏実, 森下竜一

糖尿病が脳血管認知症のみならず, アルツハイマー病 (AD) の後天的危険因子であることが報告されているが, その機序は明らかでない。われわれの作製したADと糖尿病の掛け合わせマウスは認知機能障害を早期より認め, 脳血管における炎症とベータ・アミロイド ($A\beta$) の蓄積増加, および神経におけるインスリン・シグナリングの低下が認められた。インスリン・シグナリングは脳内でさまざまな機能を有すると考えられている。認知症の病態進展における脳内インスリン抵抗性の関与および機序を明らかにすることは, 糖尿病を伴う認知症はもろんのこと, 加齢が最大の後天的危険因子である認知症の予防・治療法開発に貢献できると考えられる。

キーワード ● ベータ・アミロイド, インスリン・シグナリング, タウ, 糖尿病, 老化

はじめに

少子高齢化の進む現在社会において認知症問題は解決が待たれている。およそ20年後の2030年には認知症患者は300万人を超えると予想されており, 65歳以上の10人に1人は認知症という時代が来る。認知症の内訳はアルツハイマー病 (AD), 脳血管認知症, レビー小体型認知症が多い。ADの多くは孤発性であり, 先天的な遺伝因子 (APOE など) や後天的危険因子が知られている。そのなかで多くの疫学的研究により, 糖尿病がADの後天的危険因子の1つであることが報告されている。大規模コホート研究で知られるロツテルダム・スタディーにおいては糖尿病はADの発症リスクを2倍に増加させることが報告されており, 日本の久山町研究においても耐糖能異常はADの発症を2~4倍に増加させることが報告されている。一方で, 糖尿病はAD病理, すなわち老人斑や神経原線維変化を増加せしめるのか, という問いに, 剖検脳を用いた研

究においては一定の見解が得られていない^{1)~4)}。それではなぜ, 糖尿病はADの発症リスクを増加させるのだろうか? われわれはこの問いにアプローチするために, ADと糖尿病の掛け合わせマウスを作製し, その病態解析を行った。その結果, ADと糖尿病の掛け合わせマウスは認知機能障害をより早期より認め, 脳血管の炎症とベータ・アミロイド ($A\beta$) の蓄積増加, および神経におけるインスリン・シグナリングの低下が認められた (図1)。血管障害による虚血が認知症の病態進展に重要な役割を果たしていることは論を待たない。本稿ではこれまでの知見を紐解きながら, 認知症の病態進展におけるインスリン・シグナリングの役割を考える。

1 中枢神経系における インスリン・シグナリング

脳内においてもインスリンやインスリン受容体が存

Role of insulin resistance in the pathogenesis of dementia

Naoyuki Sato^{1) 2)}/Shuko Takeda^{1) 2)}/Kozue Uchio-Yamada³⁾/Hiromi Rakugi²⁾/Ryuichi Morishita¹⁾: Department of Clinical Gene Therapy, Osaka University Graduate School of Medicine¹⁾/Department of Geriatric Medicine, Osaka University Graduate School of Medicine²⁾/Laboratory of Experimental Animal Models, National Institute of Biomedical Innovation³⁾ (大阪大学大学院医学系研究科臨床遺伝子治療学¹⁾/大阪大学大学院医学系研究科老年・腎臓内科学²⁾/医薬基盤研究所³⁾)

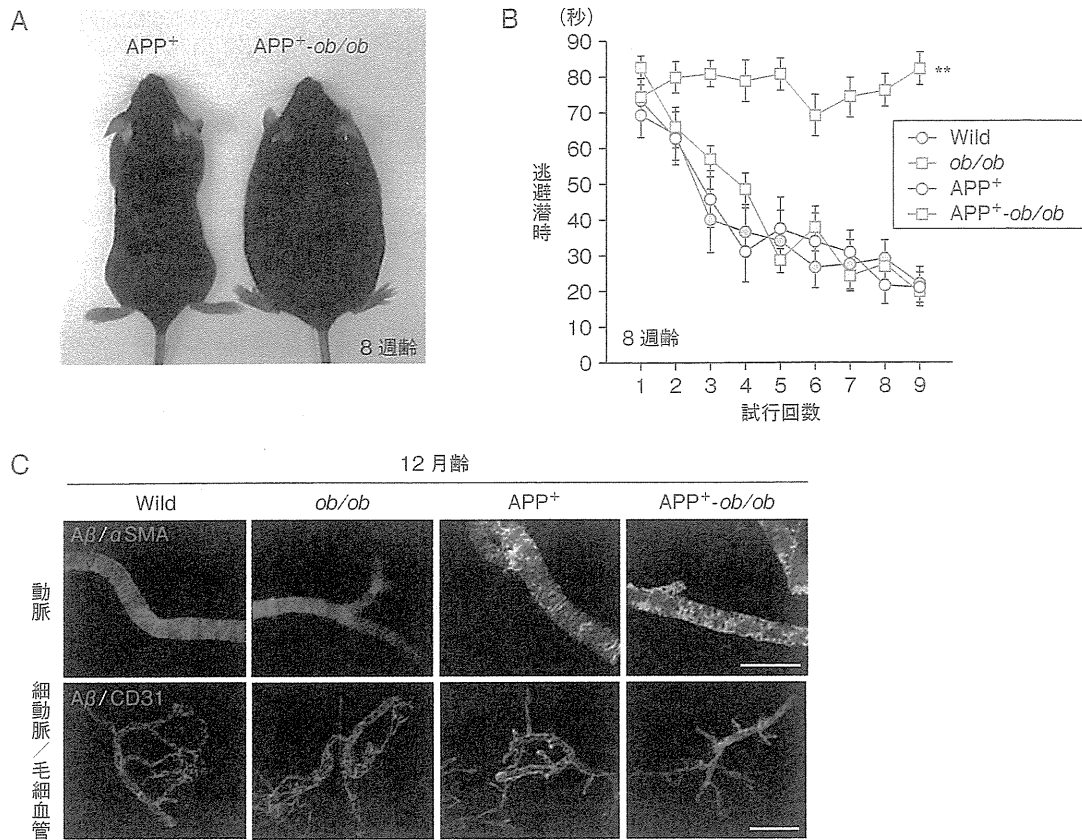


図1 糖尿病合併アルツハイマー病マウスの認知機能

A) 糖尿病合併アルツハイマー病 (AD) マウス $APP^{+}/ob/ob$. ADモデルマウス $APP23$ と ob/ob (ob/ob レプチン欠損: 高度の肥満, 高インスリン血症, 高血糖を伴う) の掛け合わせにより糖尿病合併ADマウスを作出した. B) $APP^{+}/ob/ob$ の認知機能障害 (モリス水迷路^{※1}). 生後8週という早期に認知機能障害を認めた. この週齢ではもとのADマウスは認知機能障害を呈さない. **: $p < 0.01$. C) 糖尿病合併ADマウスの脳血管のアミロイド沈着. ADモデルマウス $APP23$ はヒトの脳血管アミロイド沈着を再現しているが, 糖尿病の合併は $A\beta$ 沈着を増悪させた. α SMA: 血管平滑筋細胞マーカー, CD31: 内皮細胞マーカー. スケールバー = $100\mu m$ (A, Cは文献10より転載, Bは同文献より引用)

在し⁵⁾, 何らかの機能を担っていると考えられている⁶⁾. 実際, マウスやヒトにおいてインスリンの経鼻吸入は認知機能を高めることが報告されている⁷⁾⁸⁾. 高脂肪食を与えた動物モデルでは全身において高インスリン血症になり, このことにより血液脳関門でのインスリン・トランスポーターの発現が代償的に低下し, 脳内インスリンが低下することが報告されている⁹⁾. 前述のとおり高脂肪食により高インスリン血症にしたマウスでは, インスリンの経鼻吸入はもはや認知機能を高めることができなくなることが報告されている⁷⁾.

これらのことから糖尿病において脳内のインスリン・シグナリング・システムの機能が低下, すなわちインスリン抵抗性が生じていることが示唆される. さらにわれわれの糖尿病合併ADモデルマウスにおいても脳内インスリン・シグナリングが低下していることを確

※1 モリス水迷路

空間学習 - 記憶を評価する検査. 水を張ったプールでマウスを泳がせ, プラットホームに到達する時間を測定する. プラットホームはマウスからは見えず, マウスは周りの景色を頼りにプラットホームを探索する.

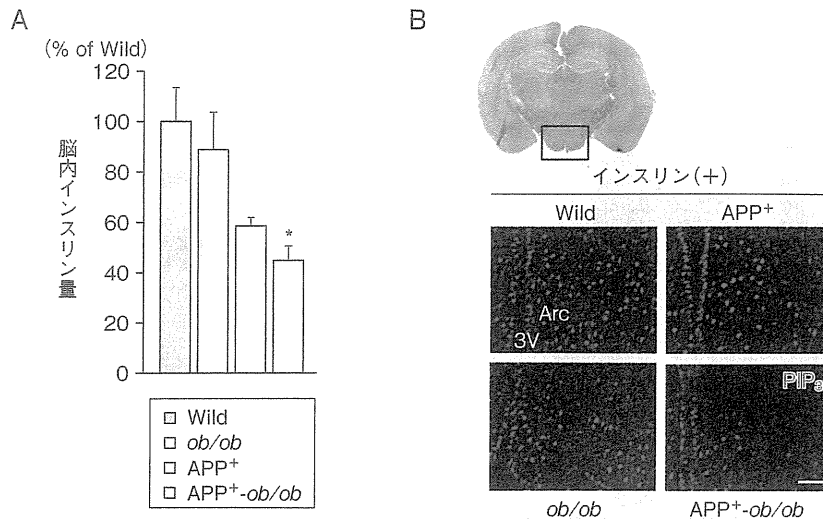


図2 糖尿病合併ADマウスの脳内インスリン量と神経細胞のインスリン・シグナリング
 A) APP⁺-ob/obマウスの脳内インスリン量。他の3群に比較し脳内インスリンはAPP⁺-ob/obマウスにおいて低下していた。*: $p < 0.05$ 。B) 脳内の神経細胞のインスリン・シグナリングの低下。腹腔インスリン注射による脳内の神経細胞のPIP₃増強がAPP⁺-ob/obマウスにおいて低下していた。PIP₃はインスリン・シグナリングにおいてIRS-2の下流でPI3Kにより産生されるセカンドメッセンジャー。3V: third ventricle (第三脳室), Arc: arcuate nucleus (弓状核)。スケールバー=100 μm (Aは文献10より引用, Bは同文献より転載)

認した(図2)¹⁰。事実、ヒトの剖検脳を用いた研究でもAD脳におけるインスリン・シグナリングの低下が示唆されている。それでは、脳内におけるインスリン・シグナリングの低下の結果、どのような機能障害が惹起されるのか? 脳内におけるインスリン・シグナリングの機能を俯瞰しながら、考えてみたい。

2 シナプス機能におけるインスリン・シグナリングの役割

インスリン受容体はシナプスに存在し、ヒトのAD患者だけでなく、正常人においてもインスリンの鼻吸入は認知機能を改善する。これらのことはインスリンが認知機能を修飾することができることを示している。その機序としてはインスリン依存性のグルコース・トランスポーターを介した機序と、インスリン・シグナリング—PI3K (phosphatidylinositol 3-kinase)—AKTを介した機序が考えられる。前者のインスリン依存性のGLUT4 (glucose transporter 4)¹¹は海馬に存

在し、脳内のインスリンは海馬においてGLUT4を活性化し、神経活動時に神経細胞内へのグルコースの取り込みを促進する¹²。一方、後者の機序として、インスリンは海馬においてPI3K—AKT—mTOR (mammalian target of rapamycin)シグナリングを活性化し、シナプス機能に重要なタンパク質の翻訳を活性化する¹³。mTORは神経細胞においてもタンパク質翻訳を制御する重要な分子であり¹⁴、例えばシナプス前においてはカリウムチャネルの¹⁵、シナプス後においてはPSD (postsynaptic density)-95のタンパク質翻訳を制御していることが報告されている¹⁶。

以上のことから、糖尿病による脳内インスリン・シグナリングの低下は神経細胞内へのグルコース取り込み低下、およびシナプス機能に重要な分子のタンパク質翻訳を低下させることで、シナプスの機能を低下させると想定される。また記憶の形成過程で海馬においてインスリン受容体¹⁷や、最近ではIGF-IIの発現が亢進することがNature誌に報告されており¹⁸、記憶の形成時に重要な役割を果たしている可能性が示唆される。

3 ADと糖尿病におけるインスリン・シグナリングの低下のメカニズム

では、どのようなメカニズムでADと糖尿病の合併においてはインスリン・シグナリングが低下するのであろうか？ 剖検脳においてはA β をも分解することが判明しているインスリン分解酵素がADにおいて増加していることが報告されている。増加したインスリン分解酵素によって脳内のインスリンが減少し、脳内のインスリン・シグナリングの低下を起こすのかもしれない。あるいは血液脳関門におけるインスリン・トランスポーターの機能低下が脳内のインスリンを減らすことに寄与しているかもしれない。実際、AD患者の脳脊髄液ではインスリン量が減少していることが報告されている。また高脂肪食負荷の動物モデルでは血液脳関門のインスリンのトランスポートが低下し、脳内のインスリンが低下することが示されている。一方、われわれの糖尿病合併ADマウスにおいてはRAGE (receptor for advanced glycation endproduct) ※2の発現増強を介して血管の炎症が惹起されており、脳内のインスリン・シグナリングが低下していた¹⁰⁾。末梢組織では炎症とインスリン抵抗性に関しては、両者が悪循環を呈することが報告されており^{19)~22)}、脳内においても血管から波及した炎症が脳内インスリン・シグナリングの低下を引き起こした可能性がある(図3)²³⁾。

4 インスリン・シグナリング、タウ、糖尿病とAD

前述のとおり、インスリン・シグナリングの下流にPI3K-AKTがあるが、このパスウェイのさらに下流にはGSK (glycogen synthase kinase) 3 β というリン酸化酵素が存在し、インスリン・シグナリングはこれを負に制御している^{24) 25)}。重要なことにこのGSK3 β はタウをリン酸化の基質としており、事実、インスリンで

※2 RAGE

慢性の高血糖は、糖がタンパク質に非酵素的に結合することを促進し最終糖化産物 (advanced glycation endproducts : AGE) を産生する。このAGEに対する受容体がRAGE (receptor for AGE) であり、イムノグロブリン・スーパーファミリーに属し、炎症反応を引き起こす。

神経細胞を刺激するとGSK3 β は抑制され、引き続いてタウのリン酸化が抑制される²⁶⁾。ここでタウのリン酸化に注目している理由は、ADの病理学的特徴である神経原線維変化がタウの異常リン酸化を伴うからである。逆に、インスリン²⁷⁾、インスリン受容体²⁸⁾、その下流のIRS (insulin receptor substrate)-2^{29)~31)}を欠失させると、タウの過剰なリン酸化が引き起こされる。これらのことから脳内のインスリン・シグナリングの低下はタウのリン酸化を亢進すると考えられる。さらに、タウのリン酸化はGSK3 β によるリン酸化と同時にPP2A (protein phosphatase 2A)による脱リン酸化によっても制御されている³²⁾。前記IRS-2の欠失はPP2Aの活性を下げることも報告されている²⁹⁾。以上のことから、糖尿病による脳内のインスリン・シグナリングの低下はGSK3 β 活性化やPP2A不活化を介して、タウのリン酸化を亢進する方向に働くと考えられる(図3)。

5 神経老化とタンパク質の折り畳み・凝集におけるインスリン・シグナリングの役割

インスリン・シグナリングが神経老化を制御するという知見がある。インスリン・IGF様シグナリングが酵母、線虫、ハエ、マウスを通じて寿命を決定することが知られている。なかでも興味深いことに、マウスにおいて中枢神経特異的にIRS-2を欠失させると寿命が延びる。このことは脳においてインスリン・シグナリングが低下すると寿命が延びることを示唆する。また、驚いたことに脳内のインスリン・シグナリングの低下は脳内A β 量を減らすことが報告されている^{30) 33)}。これらのことから、ADの剖検脳でも報告されている脳内のインスリン・シグナリングの低下は、脳老化に対する代償機構である可能性が示唆されている。しかしながら、一方でタウに関しては脳内のインスリン・シグナリングの低下は逆にそのリン酸化、すなわち異常な折り畳み・凝集を促進する方向に働く。したがって脳内のインスリン・シグナリングの低下はADの病態に対して、正と負の両方向に働いているように思える。このことは脳内のインスリン・シグナリング低下を伴う場合、認知機能を改善するためには、脳内のインスリン・シグナリングを回復すればいいのか、ある

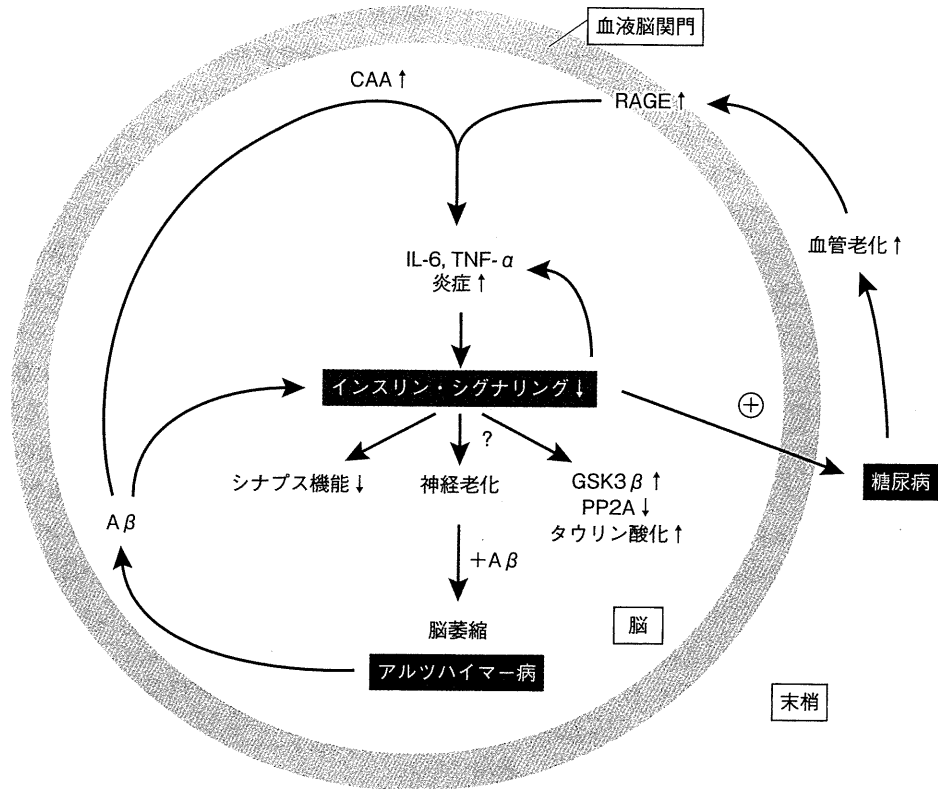


図3 脳内インスリン・シグナリングが認知機能障害をきたすメカニズム (仮説)

糖尿病では血管老化が進み、脳血管にRAGEが増加し、ベータ・アミロイド(Aβ)が蓄積しやすくなっている。RAGEの発現や血管アミロイドの増加は炎症を惹起し、脳内に波及する。炎症とインスリン抵抗性は悪循環をきたす。脳内インスリン・シグナリングの低下はシナプス機能、神経老化、タウのリン酸化に影響を与える。そのような状態にベータ・アミロイドの負荷が加わることで脳萎縮をきたす。アルツハイマー病においてベータ・アミロイドはインスリン・シグナリングの低下をきたし、脳内インスリン・シグナリングの低下は末梢において糖尿病を増悪させる。CAA: cerebral amyloid angiopathy (脳アミロイド血管症) (文献23より引用)

いはさらに抑制すればいいのか、という方向性を決定するうえで非常に重要である。

糖尿病の間にはインスリン・シグナリングを介した病態の悪循環の可能性が示唆される(図3)²³⁾。

6 ADによる糖尿病病態悪化におけるインスリン・シグナリングの役割

脳内インスリン・シグナリングの低下は全身において糖尿病を悪化させること^{34) 35)}が報告されている。また興味深いことにわれわれの糖尿病合併ADマウスにおいてもコントロールの糖尿病マウスに比べ、糖尿病の病態が増悪していた¹⁰⁾。これらのことからADと糖

■ おわりに

糖尿病による認知症の病態進展には脳内インスリン抵抗性を伴う。しかし、脳内インスリン抵抗性が病態進展を加速させているのか、あるいは脳老化に対する代償機構なのかは明らかになっていない。さらに糖尿病による認知症の病態進展にはインスリン抵抗性のみならず、血管因子も関与し、その程度および混成の度

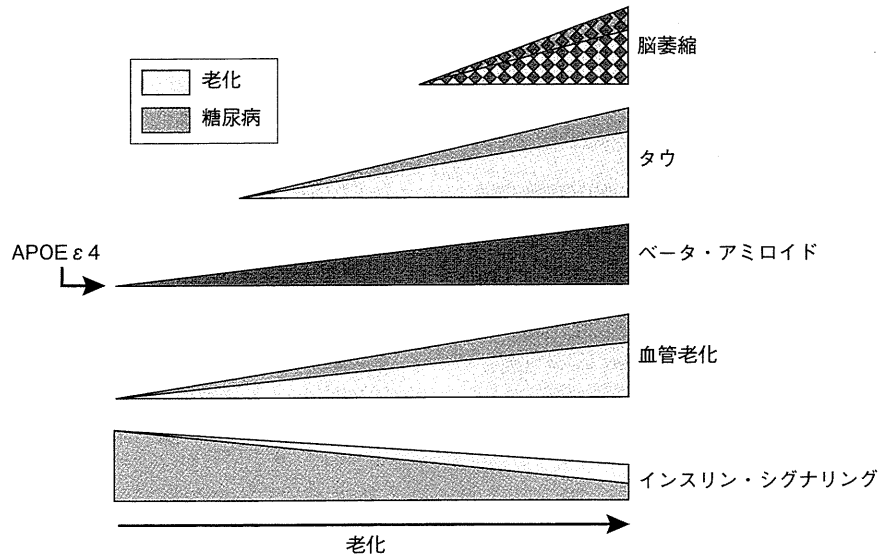


図4 認知症進展の時間軸（仮説）

老化および糖尿病により、血管の老化、インスリン・シグナリングの低下、そしてそれに引き続くタウのリン酸化が引き起こる。一方、強力な遺伝因子APOE ε 4により、ベータ・アミロイドの蓄積が促進される。これらの因子が歯車となって脳萎縮が進んでいく

合いにより、さまざまな病態を呈すると考えられ、実際の剖検脳を用いた研究をみても、その可能性を示唆するものの詳細は未だベールにつつまれている。インスリン抵抗性は加齢に伴い増大することが示唆されており（図4）、認知症の病態進展における脳内インスリン抵抗性の関与および機序を明らかにし、それらを新たな標的としてとらえることは、糖尿病を伴う認知症はもちろんのこと、加齢が最大の後天的危険因子である認知症の予防・治療開発に貢献できると考えられる。

謝辞

上田裕紀先生、藤澤智巳先生による助言、文部科学省科学研究費、科学技術振興事業団の補助にここに感謝する。

文献

- 1) Peila, R. et al. : Diabetes, 51 : 1256-1262, 2002
- 2) Matsuzaki, T. et al. : Neurology, 75 : 764-770, 2010
- 3) Kalaria, R. N. : Nat. Rev. Neurol., 5 : 305-306, 2002
- 4) Beeri, M. S. et al. : J. Gerontol. A Biol. Sci. Med. Sci., 60 : 471-475, 2005
- 5) Havrankova, J. et al. : Nature, 272 : 827-829, 1978
- 6) Wickelgren, I. : Science, 280 : 517-519, 1998
- 7) Marks, D. R. et al. : J. Neurosci., 29 : 6734-6751, 2009
- 8) Benedict, C. et al. : Psychoneuroendocrinology, 29 : 1326-1334, 2004
- 9) Kaiyala, K. J. et al. : Diabetes, 49 : 1525-1533, 2000
- 10) Takeda, S. et al. : Proc. Natl. Acad. Sci. USA, 107 : 7036-7041, 2010
- 11) Olson, A. L. & Pessin, J. E. : Annu. Rev. Nutr., 16 : 235-256, 1996
- 12) Grillo, C. A. et al. : Brain Res., 1296 : 35-45, 2009
- 13) Lee, C. C. et al. : J. Biol. Chem., 280 : 18543-18550, 2005
- 14) Parsons, R. G. et al. : J. Neurosci., 26 : 12977-12983, 2006
- 15) Raab-Graham, K. F. et al. : Science, 314 : 144-148, 2006
- 16) Scott, P. H. et al. : Proc. Natl. Acad. Sci. USA, 95 : 7772-7777, 1998
- 17) Dou, J. T. et al. : Learn. Mem., 12 : 646-655, 2005
- 18) Chen, D. Y. et al. : Nature, 469 : 491-497, 2011
- 19) Rotter, V. et al. : J. Biol. Chem., 278 : 45777-45784, 2003
- 20) Klover, P. J. et al. : Diabetes, 52 : 2784-2789, 2003
- 21) Andersson, C. X. et al. : J. Biol. Chem., 282 : 9430-9435, 2007
- 22) Campos, S. P. et al. : J. Biol. Chem., 271 : 24418-24424, 1996
- 23) Sato, N. et al. : Curr. Aging Sci., in press (2011)
- 24) Sutherland, C. et al. : Biochem. J., 296 (Pt 1) : 15-19, 1993

- 25) Cross, D. A. et al. : Nature, 378 : 785-789, 1995
- 26) Hong, M. & Lee, V. M. : J. Biol. Chem., 272 : 19547-19553, 1997
- 27) Schechter, R. et al. : Biochem. Biophys. Res. Commun., 334 : 979-986, 2005
- 28) Schubert, M. et al. : Proc. Natl. Acad. Sci. USA, 101 : 3100-3105, 2004
- 29) Schubert, M. et al. : J. Neurosci., 23 : 7084-7092, 2003
- 30) Killick, R. et al. : Biochem. Biophys. Res. Commun., 386 : 257-262, 2009
- 31) Freude, S. et al. : Curr. Alzheimer Res., 6 : 213-223, 2009
- 32) Sontag, E. et al. : Neuron, 17 : 1201-1207, 1996
- 33) Freude, S. et al. : FASEB J., 23 : 3315-3324, 2009
- 34) Gerozissis, K. : Eur. J. Pharmacol., 490 : 59-70, 2004
- 35) Obici, S. et al. : Nat. Med., 8 : 1376-1382, 2002

Profile

筆頭著者プロフィール


里 直行：兵庫県生まれ。1992年、大阪大学医学部卒業。老年医学講座大学院にて荻原俊男先生、三木哲郎先生のもとAD研究を開始。日本学術振興会特別研究員（PD）を経て、シカゴ大学のAD研究のメッカGopal Thinakaran先生、Sangram Sisodia先生の研究室に留学。帰国後もADの診断・予防・治療法の開発をめざして研究を行っている。科学技術振興財団A-STEP研究代表者。AD新規診断法の臨床研究を実施中。物忘れ外来、認知症病棟にて日々の診療を行っている。大学院生、共同研究を募集中。ホームページ（<http://www.cgt.med.osaka-u.ac.jp>）の参照をお願いします。

Book Information

がんの 分子標的と 治療薬事典

編／西尾和人
西條長宏

好評発売中



反響続々!!

- ◆ 既知情報が、一冊にまとめてあり個々の情報も簡潔に要点が記載されているので、重宝しています。(大学研究職員)
- ◆ 分子標的薬の概略と個々の薬に関する説明が充実していて理解しやすい。(大学研究職員)

分子標的治療を原理から、薬剤から、理解できる
基礎・臨床問わず必携の1冊がついに登場!!

- ◆ 定価(本体7,600円+税)
- ◆ 347頁 B5判 2色刷り
- ◆ ISBN 978-4-7581-2016-6

発行 **羊土社**

